A Conserved Disulfide Motif in Human Tear Lipocalins Influences Ligand Binding†

B. J. Glasgow,*,‡,§ A. R. Abduragimov,§ T. N. Yusifov,‡ O. K. Gasymov,‡ J. Horwitz,§ W. L. Hubbell,§,|| and K. F. Faull⊥

Departments of Pathology, Ophthalmology, Chemistry & Biochemistry, and Psychiatry & Biobehavioral Sciences and the Neuropsychiatric Institute, UCLA School of Medicine, Los Angeles, California 90095

Received August 22, 1997; Revised Manuscript Received November 19, 1997

ABSTRACT: Structural and functional characteristics of the disulfide motif have been determined for tear lipocalins, members of a novel group of proteins that carry lipids. Amino acid sequences for two of the six isolated isoforms were assigned by a comparison of molecular mass measurements with masses calculated from the cDNA-predicted protein sequence and available N-terminal protein sequence data. A third isoform was tentatively sequence assigned using the same criteria. The most abundant isoform has a measured mass of 17 446.3 Da, consistent with residues 19−176 of the putative precursor (calculated mass 17 445.8 Da). Chemical derivatization of native and reduced/denatured protein confirmed the presence of a single intramolecular disulfide bond in the native protein. Reactivity of native, reduced, and denatured protein with 4-pyridine disulfide and dithiobis(2-nitrobenzoic acid) indicated that access to the free cysteine is markedly restricted by the intact disulfide bridge. Mass measurements of tryptic fragments identified C_{119} as the free cysteine and showed that the single intramolecular disulfide bond joined residues C_{79} and C_{171}. Circular dichroism indicated that tear lipocalins have a predominant β-pleated sheet structure (44%) that is essentially retained after reduction of the disulfide bond. Circular dichroism in the far-UV showed reduced molecular asymmetry and enhanced urea-induced unfolding with disulfide reduction indicative of relaxation of protein structure. Circular dichroism in the near-UV shows that the disulfide bond contributes to the asymmetry of aromatic sites. The effect of disulfide reduction on ligand binding was monitored using the intrinsic optical activity of bound retinol. The intact disulfide bond diminishes the affinity of tear lipocalins for retinol and restricts the displacement of native lipids by retinol. Disulfide reduction is accompanied by a dramatic alteration in ligand-induced conformational changes that involves aromatic residues. The disulfide bridge in tear lipocalins is important in conferring protein rigidity and influencing ligand affinity. The disulfide bond appears highly conserved so that these findings may have implications for the entire lipocalin superfamily.

The corneal surface is continually bathed in tears which are secreted by the lacrimal glands. This surface is directly exposed to the outside environment and lacks a blood supply. Therefore, the cornea requires oxygen diffusion from the air, protection from dehydration and infection, and simultaneous maintenance of optical clarity. The tear film is essential for satisfying these requirements. Tear lipocalins (TL),[1] recently recognized members of the lipocalin family, comprise 15−33% of the protein content of tears (*1*−*3*). TL bind a broad array of lipid molecules including cholesterol, fatty acids, phospholipids, and glycolipids that are surface active and/or antimicrobial (*4*). Therefore, TL may act as a lipid carrier in tears and scavenge lipid from the corneal surface or provide a reservoir of lipid molecules that upon release migrate to the film surface where they reduce water evaporation and inhibit microbial infection of the exposed ocular surface.

Lipocalins are a widely distributed class of lipid carrier proteins characterized by sequence homology of specific conserved regions and a predominantly pleated β-sheet secondary structure (*5*). Homology and mapping studies link TL to the lipocalin family (*6*, *7*). However, unlike most members of this family, TL bind a broad array of lipid molecules (*4*). This broad ligand specificity must be conferred by unique structural properties. A β-sheet secondary structure of TL has been predicted by analogy with lipocalin structure and more specifically from hydropathy

† Grant support: Karl Kirschgessner, Stein-Oppenheimer, and W. M. Keck Foundations, an unrestricted grant from Research to Prevent Blindness, and USPHS NIH EY 11224 and EY 00331.

* Author to whom correspondence should be addressed.
‡ Department of Pathology.
§ Department of Ophthalmology.
|| Department of Chemistry & Biochemistry.-
⊥ Department of Psychiatry & Behavioral Sciences and the Neuropsychiatric Institute.

[1] Abbreviations: a, average (chemical calculation of mass); CD, circular dichroism; CZE, capillary zone electrophoresis; Da, dalton (one twelfth the mass of ^{12}C); DTNB, Dithiobis(2-nitrobenzoic acid); DTT, dithiotreitol; EDTA, ethylenediaminetetraacetic acid; ESI, electrospray ionization mass spectrometry; FIA-ESI, combined flow injection−electrospray ionization mass spectrometry; GHCl, guanidine hydrochloride; HPTL, highly purified tear lipocalins; IAA, iodoacetic acid; LC-ESI, combined liquid chromatography−electrospray ionization mass spectrometry; m, monoisotopic (calculation of mass); MALDI, matrix-assisted laser desorption ionization mass spectrometry; mdegrees, millidegrees; MH^+_c, molecular weight (chemical) of the singly charged protonated molecule; MH^+_m, molecular weight (monoisotopic) of the singly charged protonated molecule; MS/MS, tandem mass spectrometry; PAGE, polyacrylamide gel electrophoresis; PDS, 4-pyridine disulfide; PTL, purified tear lipocalins; RP-HPLC, reverse phase high-performance liquid chromatography; TL, tear lipocalins; RPTL, reverse phase purified tear lipocalins; 4VP, 4-vinylpyridine.

S0006-2960(97)02088-6 CCC: $15.00
Published on Web 02/06/1998

profiles and analysis from the deduced linear sequence (*1*), although direct proof of TL secondary structure is lacking.

The TL cDNA-deduced amino acid sequence suggests the precursor protein is 176 residues in length (*1*). N-Terminal amino acid sequencing has shown the purified protein begins at residue 19 (*1, 2, 8, 9*), suggesting precursor truncation occurs during expression. Additionally, up to 12 different N-terminal amino acid sequences have been reported (*9*), suggesting variability in N-terminal processing is responsible for at least some of the heterogeneity in the expressed protein.

The number of disulfide bridges in several lipocalins has been deduced (*10*). Most lipocalins are presumed to have one or two intramolecular disulfide bonds. Exceptions include retinol binding protein, which has three, bovine odorant binding protein, which does not have any (*10*), and apolipoprotein D, which forms intermolecular disulfide bonds (*11*). In nearly all of the lipocalins with disulfide bridges, there is a conserved intramolecular disulfide bond involving the carboxy-terminal end. With only three cysteines by amino acid analysis and as predicted by the cDNA sequence (*1, 2, 3, 10, 12*), TL could potentially contain only one intramolecular disulfide bond. Therefore, TL are potential candidates to study the structural changes conferred by this conserved disulfide bond with implications for the entire lipocalin family.

Lipid binding and transport proteins are essential in the maintenance of cellular and bodily function. Detailed biophysical investigations of these proteins are necessary to understand their structure, specificity, and modes of action. We describe the precise mass of the major species of TL and the number and positions of free and disulfide-linked cysteines in TL. We characterized the secondary structure in TL and investigated the role of the disulfide bond in maintaining the secondary structure as well as conformational alterations during retinol binding. The results of these experiments demonstrate the role of the disulfide bond and provide the foundation for studying molecular mechanisms of ligand binding by this class of proteins.

EXPERIMENTAL PROCEDURES

Reagents. Trifluoroacetic acid, acetonitrile, HPLC grade water, DTT, and GHCl were purchased from Fisher, 4VP was purchased from Aldrich, PDS, DTNB, trypsin (type XIII), and all trans-retinal were purchased from Sigma, and urea (ultrapure) was purchased from Schwarz/Mann Biotech. All other reagents and solvents were of analytical grade or better.

Tear Lipocalin Purification. Three different samples of TL were used. PTL were produced from pooled human tear samples by size exclusion and ion exchange column chromatographies as previously described (*4, 9*), HPTL were produced from PTL by an additional C_4 RP-HPLC step, and RPTL were produced directly from freshly collected tears by a single step of C_8 RP-HPLC. Delipidation was performed as described previously by chloroform/methanol extraction (*4*). Protein concentrations were determined by the Biuret method (*13*). Purity of the final samples was assessed by a combination of techniques including analytical SDS tricine PAGE (*4*), the profile of 215 nm absorption following CZE and RP-HPLC, and the pattern of ions produced by MALDI and ESI mass spectrometry.

High-Pressure Liquid Chromatography. Tear and PTL samples dissolved in aqueous TFA (0.1%) were separated by RP-HPLC using an increasing linear gradient of acetonitrile in water, both containing 0.1% TFA. For the preparation of HPTL, Shandon Hypersil C_4 (10 μm particle size, 300 Å pore diameter, 250 × 2.1 mm, 400 μL/min), and Vydac C_4 (10 μm particle size, 300 Å pore diameter, 250 × 4.6 mm, 1 mL/min) columns were used with equivalent results. For the preparation of RPTL a Vydac C_8 (5 μm particle size, 300 Å pore diameter, 250 × 4.6 mm, 1 mL/min) column was used. For the purification of tryptic fragments a Keystone C_8 (BetaBasic-8, 5 μm particle size, 300 Å pore diameter, 250 × 4.6 mm, 1 mL/min) column was used. Eluate absorbance at 215 and/or 280 nm was monitored and fractions (typically 1 min duration) were collected for subsequent analysis.

For LC-ESI with reverse phase resins the same solvents were used with microbore columns (100 × 1 mm, 40 μL/min). Native and chemically modified HPTL was chromatographed on C_4 (Shandon Hypersil) and C_8 (Brownlee Aquapore) resins which gave similar chromatographic resolution for the same samples except a higher concentration of acetonitrile was necessary for elution from the octyl column. Trypsin digests were chromatographed on a C_{18} resin (Keystone Betasil C_{18}, 100 × 1 mm, 5 μm particle size, 100 Å pore diameter, 40 μL/min). For rapid desalting prior to ESI, samples were injected onto a microbore size exclusion column (TosoHass TSK HSW 40, 45 or 20 × 1 mm) which was equilibrated and eluted isocratically (10 μL/min) with water/acetonitrile/formic acid (50/50/0.1). In each case the column effluent was monitored for absorbance at 215 nm and then passed directly into the electrospray ion source.

Electrospray Mass Spectrometry. A Perkin-Elmer Sciex (Thornhill, Canada) API III triple quadrupole mass spectrometer was calibrated by flow injection of a mixture of polypropylene glycol (PPG) 425, 1000, and 2000 (3.3×10^{-5}, 1×10^{-4}, and 2×10^{-4} M, respectively) in water/methanol (1/1, v/v) containing 2 mM ammonium formate and 0.1% acetonitrile. Normal spectra were obtained by scanning at instrument conditions sufficient to resolve the isotopes of the PPG/NH_4^+ singly charged ion at *m*/*z* 906 with 40% valley and with a 0.3 Da step size during data acquisition. An orifice voltage of 90 was used for analysis of proteins, and for the analysis of proteolytic digests the orifice was either ramped from 50 to 120 V with mass or held constant at 50 V. MS/MS daughter ion spectra were obtained after detuning the mass spectrometer (to increase sensitivity) such that the isotopes of the PPG-NH_4^+ singly charged ion at *m*/*z* 906 were not resolved from one another. The nomenclature used when referring to daughter ions as the Y-, B-, or C-type ions refers to N-terminal fragments (B and C type) and C-terminal fragments (Y type) according to Roepstorff and Fohlman (*14*) and Biemann (*15*). For FIA, samples dissolved in water/acetonitrile/formic acid (50/50/0.1) were injected into a stream of the same solvent entering the electrospray source (10 μL/min). Deconvolution of the series of multiply charged ions found in normal spectra and calculation of peptide or protein molecular weight was achieved with the Hypermass computer program supplied with the instrument. The prediction of possible daughter ions formed during MS/MS from parent peptides was made using

the MacBiospec computer program supplied with the instrument.

Laser Desorption Mass Spectrometry. Spectra were recorded with a reflector time-of-flight instrument (PerSeptive Biosystems Voyager RP), used in the linear mode with α-cyano-4-hydroxycinnamic acid matrix unless otherwise stated. Calibration was performed with horse heart myoglobin (external) and bovine insulin (internal).

Capillary Zone Electrophoresis. Samples dissolved in conducting solution (100 mM sodium phosphate, pH 2.3) were injected (1 nL) into a 50 cm × 50 μm capillary and electrophoresed at 21 kV for 1 h (Beckman P/ACE System 5000) with 214 nm recording of the eluate.

Protein Pyridoethylation. Tears were treated within 30 s following collection with 4VP (1 μL of 4-VP/100 μL of tears, 1 h, 23 °C). Following centrifugation the supernatant was either frozen before chromatography or subjected immediately to C_8 RP-HPLC.

HPTL (250 pmol) in Tris−HCl buffer (100 μL, 150 μM, pH 8.4) was treated with 4VP (1 μL, neat or diluted in water, room temperature, 1 h) following which β-mercaptoethanol was added (2 μL, 28.4 μmol) and the reaction mixture was analyzed by LC-ESI. These experiments were also done by first treating the protein with GHCl (aqueous 6 M containing 100 mM sodium phosphate, pH 7.7) prior to the addition of 4VP.

Pyridoethylation was also carried out with HPTL that had been first treated with DTT and GHCl. Dried protein (250 pmol) was redissolved in GHCl (6 M, 10 μL, containing 100 mM sodium phosphate, pH 7.7) and to which was added DTT (20 nmol in 2 μL of water). After 1.75 h at room temperature 4VP was added (1 μL, neat, 9.3 μmol). After another hour at room temperature β-mercaptoethanol was added (3 μL, neat, 42.6 μmol), and the reaction mixture was analyzed by LC-ESI.

Reaction with Iodoacetic Acid. Dried HPTL (250 pmol) was redissolved in aqueous GHCl (6 M, 10 μL) to which was added additional buffer (Tris−HCl, 0.5 M, pH 8.6, 10 μL) and DTT (20 nmol in 2 μL of water). After 1.75 h at room temperature iodoacetic acid was added (200 nmol in 20 μL of water). After an additional 15 min at room temperature β-mercaptoethanol was added (5 μL, neat, 71 μmol) and the reaction mixture was purified by RP-HPLC for analysis by FIA-ESI.

Trypsin Digestion. HPTL samples (2.6 nmol) were redissolved in freshly prepared aqueous urea (8 M, 100 μL), and the solution was left at room temperature for 3.5 h following which additional water was added (350 μL, final urea concentration 1.8 M) and the sample was mixed with HPLC-purified trypsin, type XIII (400 pmol, in ammonium bicarbonate, 50 mM, pH 8.1) (*14*), and incubated (37 °C, 15 h). Dried RPTL samples were redissolved in freshly prepared aqueous urea (8 M, 50 μL), and the solution was left at room temperature for 3−5 h following which Tris−HCl buffer was added (25 mM, pH 8.5, 200 μL, final urea concentration of 1.6 M) containing HPLC-purified TPCK-treated trypsin (TL/trypsin molar ratio between 10 and 40/1) and incubated (23 °C, 13.5−16 h). At various intervals aliquots (10 μL) of some digests were examined by microbore size exclusion LC-ESI to determine the extent of digestion. The digests were dried and redissolved (0.1% TFA, 80 μL) and aliquots (20 μL, equivalent to 650 pmol of TL) were analyzed by LC-ESI.

Preparation of Reduced PTL for Chemical Determination of Sulfhydryls and CD Analysis. Dried PTL were dissolved in 6 M GHCL containing 100 mM Tris−HCl pH 8.0 and 50 mM DTT. After 2 h of incubation at room temperature, the reduced sample was applied to a column of Sephadex G-25, $V = 5$ mL, $D = 0.5$ cm, and 0.9 mL fractions were collected. The elution buffers for experiments using 4-pyridine disulfide, DTNB, and CD, were 10 mM potassium phosphate, pH 7.4, 6 M GHCL, 100 mM Tris−HCl pH 7.3, 1 mM EDTA; and 25 mM Tris HCl, pH 8.4, 0.5 mM mercaptoethanol, respectively.

4-Pyridine Disulfide Determination of Protein Sulfhydryl Content. PTL (28.5 nmol) and reduced PTL (see above, 12.5 nmol) were redissolved in potassium phosphate buffer (500 μL, 10 mM, pH 7.4) and treated with pyridine disulfide solution (500 μL, 2 mM in 10 mM potassium phosphate, pH 7.4). After 60 min of incubation at room temperature the resulting thiopyridone was measured by recording the absorbance of the solution at 324 nm. The sulfhydryl group/protein molar ratio was calculated using the thiopyridone molar extinction coefficient of 1.98×10^4 (*17*).

Dithiobis(2-nitrobenzoic acid) Determination of Protein Sulfhydryl Content. PTL (28.5 nmol) and reduced PTL (17.2 nmol, see above) were redissolved in GHCl (950 μL, 6 M, in 100 mM phosphate buffer, pH 7.3, and 1 mM EDTA) and treated with DTNB solution (50 μL, 3 mM in 100 mM potassium phosphate, pH 7.3). The 412 nm absorbance increase was recorded at 25 °C (*18*). The sulfhydryl group/protein molar ratio was calculated using the nitrothiobenzoate molar extinction coefficient of 1.37×10^4 (*19*).

Preparation of Retinol-TL Complex. Retinol was obtained by reduction of all-trans retinal with sodium borhydride as previously described (*20*). The concentration of retinol was determined from absorbance at 325 nm using a molar extinction coefficient of 5.3×10^4 (*21*). PTL and reduced PTL (70 nmol) in Tris−HCl (1.2 mL, 25 mM, pH 8.4) without and with β-mercaptoethanol (140 nmol), respectively, were incubated with retinol (2 μL, 70 mM solution in ethanol) at 22 °C, 30 min, and used in CD spectral analysis.

Circular Dichroic Spectral Measurements. Spectra were recorded (Jasco 600 spectropolarimeter, 0.2 mm path length for far-UV spectra and 10 mm path length for near-UV spectra) using PTL protein concentrations of 1.2 mg/mL. Eight or 16 scans for the 190−260 and 250−420 nm wavelength ranges were averaged, respectively. Results were recorded in millidegrees. Computer-assisted estimation of α-helix and β-sheet content in TL was made using the self-consistent method, including the Johnson, Karbsch−Sandars and Levitt−Greer formulas (*22*).

RESULTS

Mass Spectrometric Characterization of PTL and HPTL. RP-HPLC of ion exchange and size exclusion purified TL (PTL) showed a predominant asymmetric peak of 215 nm absorption eluting at approximately 38% acetonitrile from the C_4 column accompanied by some smaller later eluting peaks (Figure 1A). CZE analysis of a similar PTL preparation showed a single asymmetric peak of 215 nm absorption suggesting the sample consisted of a major and several minor

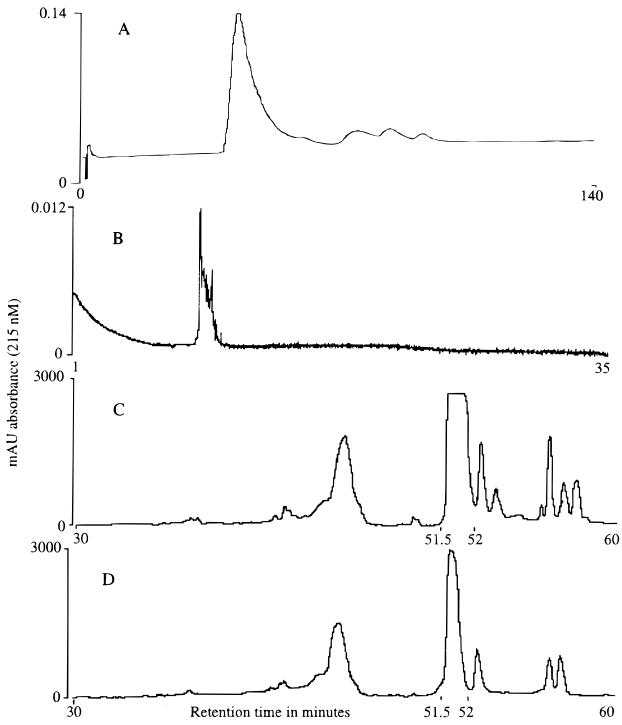

FIGURE 1: (A) Elution profile of PTL (1.4 nmol) from C_4 RP-HPLC. (B) CZE analysis of PTL. (C) Elution profile of untreated tears (350 μL) from C_8 RP-HPLC. (D) Elution profile of 4VP-treated tears (350 μL) from C_8 RP-HPLC.

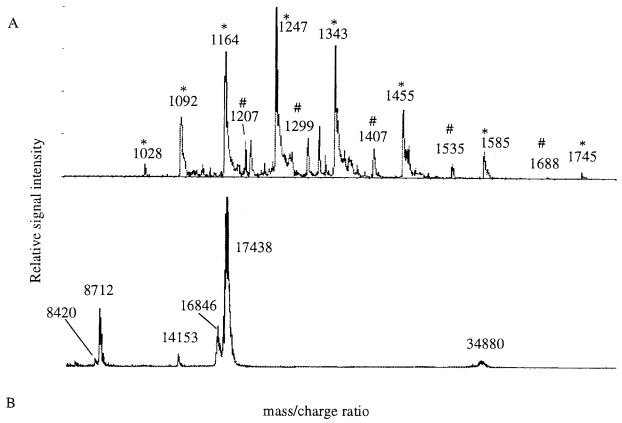

FIGURE 2: (A) Electrospray mass spectra of the peak fraction from RP-HPLC purified protein (HPTL) in Figure 1A. Deconvolution of the signals reveals a predominant component (*) of mass 17 447.8 Da and a minor component (#) of mass 16 875.7 Da. (B) Laser desorption mass spectrum of PTL (3 pmol of protein with sinapinic acid as matrix and external calibration) shows the singly and doubly charged ions for the major component at *m*/*z* 17 438 and 8712, the corresponding ions for the minor component at *m*/*z* 16 846 and 8420, an ion corresponding to a dimer of the major component at *m*/*z* 34 880, and an impurity at *m*/*z* 14 153.

components of similar electrophoretic mobility (Figure 1B). ESI on fractions collected across the RP-HPLC peak revealed the sequential elution of molecules of similar mass presumably representing various TL isoforms (Figure 2A). MALDI performed on PTL samples showed intense peaks consistent with monomeric TL and minor signals (less than 5% of the signal for the monomer) at the position of the dimer (Figure 2B). The relative heights of the minor signals were uninfluenced by the prior addition of DTT.

Analyses of multiple PTL and HPTL preparations by ESI revealed the consistent appearance of six isoforms of TL (Table 1), the most abundant component of which accounted for approximately 60−70% of the total mass spectrometric response. The mass measurements of the two most abundant forms agreed within experimental error with the calculated mass of residues 19−176 and 24−176, derived from the putative precursor (Figure 2 and Table 1) (*1*, *2*, *6*, *7*, *9*). The mass of a third isoform was consistent with the mass predicted from a previously published sequence with inclusion of an additional phenylalanine residue (Table 1) (*2*). With a mass measurement accuracy of less than or equal to 0.017% (footnote Table 1) a distinction cannot be made between forms without and with one internal disulfide bond (mass difference of 2 Da equivalent to 0.011% of the molecular weight) even if the protein were homogeneous for disulfide bond content. Therefore, more detailed experiments were conducted to resolve this question and to define the residues involved in any internal disulfide bond.

Disulfide Quantitation of PTL. Experiments with PDS and DTNB on PTL demonstrated that in the fully reduced state TL contained three free sulfhydryl groups (Table 2). However, in these experiments with nonreduced protein the molar ratio of sulfhydryl groups per mole of TL was not an integer.

4-Vinylpyridine and Iodoacetic Acid Reactivity of HPTL. Experiments which varied the molar ratio of 4VP to HPTL gave clearest results with ratios between 3700 and 370. The results of one such experiment (Table 3) show that the four identifiable forms of the native protein increased in mass by about 105−107 Da following 4VP treatment. Similar results were obtained with and without prior treatment of the protein with GHCl. However, reaction of GHCl- and DTT-treated HPTL with 4VP resulted in about a 3-fold greater mass increase. Experiments with IAA were less successful because of the formation of multiple products. The results of one these experiments (Table 3) showed that the reaction of GHCl- and DTT-treated HPTL with IAA resulted in a mass increase of 177.6 Da in the most abundant product. However, this spectrum was quite complex and showed evidence for the presence of at least 11 products following IAA treatment.

Trypsin Digestion of HPTL. Overnight trypsin digestion of HPTL using molar ratios of trypsin/substrate of 1:6.5 produced a range of fragments which were readily resolved and mass measured by RP-HPLC-ESI (Figure 3A). Three separate trypsin digestions of HPTL were carried out, and essentially identical results were obtained from all three. Molecular weight based searches for predicted trypsin fragments of TL revealed the presence of cleavages at all 7 of the available arginine residues and 9 of the available 11 lysine residues (Lys_{94} and Lys_{112} missed). A map of those peptides found in the digests which correspond to predicted tryptic fragments of TL_{19-176} is presented in Figure 4. The observed tryptic fragments cover all but eight of the 157 residues of the protein (94.9% coverage, Pro_{127}−Arg_{129} and Ala_{151}−Arg_{155} not accounted for), the relatively small missing fragments may have emerged in the nonretained portion of the HPLC chromatogram and were consequently lost in the high ion current present at that time. The molecular weight based search for predicted tryptic fragments revealed only one containing Cys_{119} which, without any additional data, was tentatively assigned to the Ser_{109}−Lys_{126} fragment (Figure 3B). In none of the tryptic digests was evidence obtained for peptides containing Cys_{79} or Cys_{171}. Searches

Table 1: Molecular Weights of TL as Determined by Electrospray Mass Spectrometry[a]

components by decreasing relative abundance	electrospray measured mass Da[b]	mass inferred from cDNA[c]	putative protein fragments[d]
RPTL and HPTL protein			
major	17 446.3 ± 2.2, $n = 12$	17 445.8	19−176
minor	16 872.75 ± 0.4, $n = 6$	16 874.1	24−176
minor	17 476.48 ± 2.2, $n = 5$	17 474.9	TL 18/5.2 + Phe[e]
minor	17 416.3 ± 1.3, $n = 2$		
minor	17 521.1 ± 0.8, $n = 2$		
minor	17 557.2 $n = 1$		
RPTL protein[f]			
major	17 441.6	17 445.8	19−176
minor	16 870.3	16874.1	24−196
minor	15 524.4		

[a] The mean of 19 different measurements of horse heart myoglobin (used as a calibration check during the collection of the data) molecular weight was 16 951.7 ($n = 19$, standard deveation = 1.3), and the highest and lowest of these values were 0.011% and 0.017% different from the actual molecular weight (16 951.5 Da), respectively. [b] Average of all the fractions in which this isoform was detected (mean ± standard deveation, n). [c] Calculated molecular weight for the fully reduced form (three free cysteines). [d] Numbered according to published cDNA sequence (*1*). [e] Calculated as TL 18/5.2 (*2*) with insertion of an additional phenylalanine. [f] This sample was obtained from two donors, and the data represent single measurements made on the pooled sample.

Table 2: Spectrophotometric Determination of Molar Cysteine Ratio in TL

sample	reagent	molar ratio of sulfhydryl groups/mol of lipocalin
PTL	PDS	0.26
denatured and reduced PTL[a]	PDS	3.05
denatured PTL	DTNB	0.11
denatured and reduced PTL	DTNB	2.91

[a] See methods.

for tryptic peptides involving single disulfide bonds and all combinations of the three available cysteines revealed in all three digests a signal for a peptide of mass 1612.7 Da which would correspond to Cys_{79}−Lys_{83} joined to Gln_{167}−Asp_{176} (Figure 3C). Treatment of one of the trypsin digests with a molar excess of DTT immediately prior to injection on the HPLC column resulted in the complete disappearance of this fragment.

Mass Spectrometric Characterization of RPTL. ESI on the major fraction (retention time 50.5−52 min) collected during the C_8 RP-HPLC of untreated tears (Figure 1C) revealed the elution of molecules of measured molecular weights of 17 524.4, 17 441.6, and 16 870.3 Da (in relative abundances of 17/100/30, respectively, based on ion current intensites). These molecules were indistinguishable on the basis of molecular weight from the major and two of the minor proteins found in the PTL and HPTL samples (Table 1), and which together accounted for about 52% of the total ion current intensity in the sample.

ESI on the peak (retention time 50.5−52 min) collected from 4VP-treated tears (Figure 1D) revealed the elution of molecules with measured molecular weights of 17 549.4 and 16 976.7 Da (in relative abundances of 100/12, respectively, based on ion current intensites), which were indistinguishable on the basis of molecular weight from the two major peaks seen in 4VP-treated HPTL (Table 3) and which together accounted for about 79% of the total ion current in the sample. In these samples ions from non-4VP-reacted molecules could not be detected, suggesting virtually complete derivatization of the protein had taken place. The observed molecules are respectively 107.7 and 106.4 Da heavier than the counterparts found in non-4VP-treated tears and represent the addition of one 4VP moiety to each molecule.

Trypsin digestion of RPTL prepared from tears with and without prior 4VP treatment produced a similar but not identical map of peptides to that produced from HPTL (the results from three trypsin digestion experiments are summarized in Table 4). The differences between the three digestions are most likely due to the presence or absence of 4VP treatment and to the slightly different trypsinization conditions used in the various experiments (substrate/trypsin ratio and time of incubation). Both the RPTL and RPTL−4VP preparations yielded a peptide of about 1613 Da characterized during LCMS by an intense doubly charged ion at m/z 807 with less intense singly and triply charged ions at m/z 1614 and 539, respectively. This spectrum was indistinguishable from one obtained from trypsin digestion of HPTL (Figure 3C). A fraction enriched in this peptide was obtained for further study by C_8 RP-HPLC purification from trypsin digestion of RPTL and RPTL−4VP samples. Molecular weight confirmation was obtained by MALDI which showed the expected signal at m/z 1615.3 (internal calibration) corresponding to the singly charged molecular ion (calculated $MH^+_a = 1614.7$). Examination of the enriched fraction by LC-ESI showed a complete disappearance of ion at m/z 807 after treatment with DTT (molar excess of thiol reagent in aqueous 0.1% TFA, 23 °C, 1 h) and coincidental appearance of signals at m/z 606.3 and 1010.4 Da corresponding to the MH^+ ions for the two predicted individual fragments (calculated MH^+_m 79−83 = 606.3, 167−176 = 1010.4). When the enriched sample was reconstituted in water/acetonitrile/formic acid (50/50/0.1), the relative intensity of the ions in the ESI spectrum of the putative disulfide-linked peptide changed so that the triply charged ion at m/z 538 became dominant. Examination of the enriched fraction by FIA-ESI before and following DTT treatment confirmed the earlier LCMS result and showed that treatment in 43 mM DTT at 60 °C for 50 min in water/acetonitrile/formic acid (50/50/0.1) resulted in significant reduction of the parent ion intensity with coincidental appearance of ions at m/z 606.3 and 1010.1 (spectra D and E of Figure 3).

Repeated attempts to obtain a MS/MS spectrum of this disulfide-linked dipeptide from collisionally activated dissociation of the doubly and triply charged parent ions failed to produce daughter ions recognized as those expected from

Table 3: Chemical Derivatization of TL with 4-Vinylpyridine and Iodoacetic Acid

sample	initial mass	mass after thiol reagent	measured mass difference	theoretical mass difference[c]
HPTL treated with 4VP[a]	17 447.41	17 552.91	+105.5	+105.1
	17 493.67	17 600.71	+107.04	+105.1
	17 522.91	17 628.65	+105.74	+105.1
	16 878.9	16 979.58	+105.08	+105.1
RPTL	17 441.6	17 549.4	+107.7	+105.1
	16 870.3	16 976.7	+106.4	+105.1
HPTL treated with guanidine + DTT and then 4VP[b]	17 450.16	17 761.64	+315.86	+315.3
HPTL treated with guanidine + DTT and then IAA[b]	17 443.1	17 620.73	+177.63	+174.0

[a] Signals for four of the TL isoforms were assignable in this experiment. [b] Signalsfor only the major TL isoform were assignable in these experiments. [c] Assuming three reactive thiol groups after DTT treatment, otherwise one reactive thiol group.

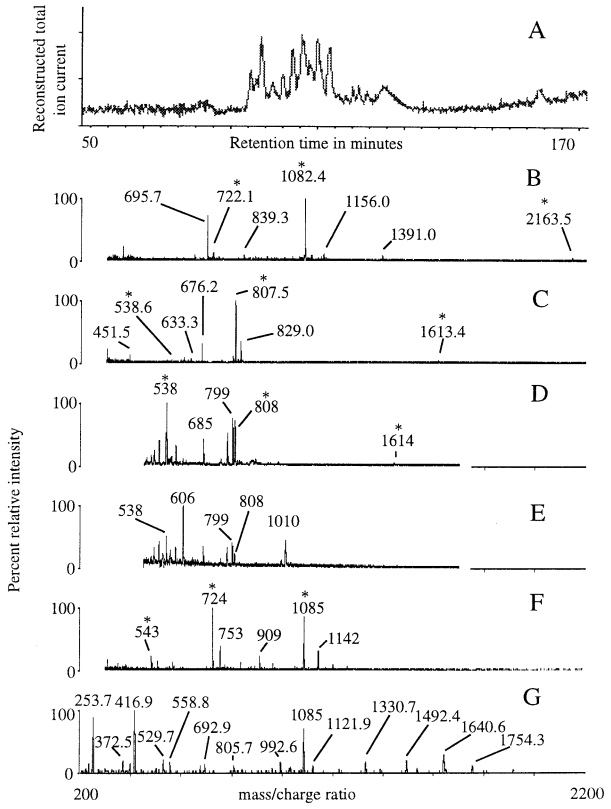

FIGURE 3: (A) Elution profile of trypsin digested HPTL (650 pmol) from C_{18} RP-HPLC. (B) Electrospray mass spectrum derived from (A) of putative tryptic fragment Ser_{109}-Lys_{126} containing Cys_{119}. *Three estimates of compound mass gave a mean result of 2162.5 Da. Calculated mass = 2162.4_a Da. (C) Electrospray mass spectrum derived from (A) of the putative disulfide linked tryptic fragment (Cys_{79}-Lys_{83}) + (Gln_{167}-Glu_{176}). *Three estimates of compound mass gave a mean result of 1612.7 Da. Calculated mass = 1612.7_m Da. (D and E) FIA-ESI mass spectra of a C_8 RP-HPLC purified fraction of an RPTL trypsin digest before (D) and following (E) DTT treatment. *Three estimates of compound mass gave a mean result of 1612.7 Da. Calculated mass = 1612.7_m Da. (F) LC-ESI mass spectrum derived from RPTL−4VP trypsin digestion showing putative Glu_{113}-Arg_{129}-4VP fragment. *Three estimates of compound mass gave a mean result of 2168.7 Da. Calculated mass = 2168.5_a Da. (G) MS/MS spectrum of daughter ions produced from *m*/*z* 1085 parent shown in (F). The ions labeled from low to high *m*/*z* are assigned the following structures with their calculated$_a$ masses: B_2 (253.2), Y_3 (371.5), B_3 (416.4), B_4 (529.6), Y_5 (556.7), Y_6 (693.8), Y_7 (807.0), Y_9 (993.2), parent, Y_{10} (1122.3), Y_{11} (1330.6), Y_{12} (1493.7), Y_{13} (1640.9), Y_{14} (1754.1).

either of the predicted peptide components (in particular B- and Y-type fragment ions, data not shown). However, MS/MS on the ions at *m*/*z* 606 and 1010 formed after DTT treatment of the putative disulfide-linked parent molecule

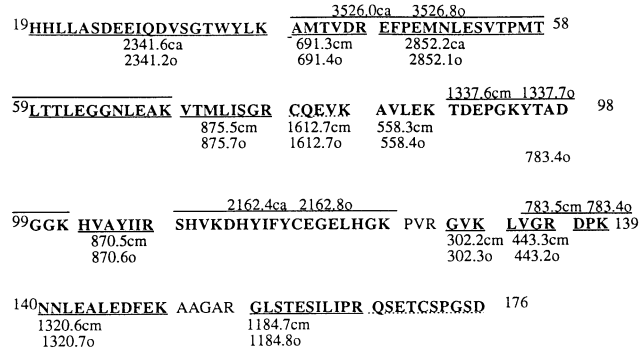

FIGURE 4: Composite primary sequence map of HPTL tryptic peptides detected by LC/ESI. Underlined segments represent those tryptic fragments that were found, dotted underlined segments were found joined by a disulfide bond. The corresponding molecular weights (Da) are given for observed (o) and calculated average (ca) and calculated monoisotopic (cm) values. Under the data acquisition parameters employed (mass step size 0.3 Da) the accuracy of mass assignment is usually $\leq \pm 1$ Da for tryptic fragments that typically yield singly, doubly, and occasionally triply charged ions.

revealed signals attributable to the presence of intense Y_1, Y_2, B_2, and B_3 daughter ions from the *m*/*z* 606 parent and intense Y_7, B_6, C_4, and Y_4 daughter ions from the *m*/*z* 1010 parent (Table 5), further confirming the assignments of the structures of these fragments.

RPTL trypsin digestion did not yield a discernible signal for a free Cys_{119}-containing peptide, but a strong signal for the corresponding pyridoethylated Cys_{119}-containing fragment 113−129 was found in the RPTL−4VP digestion (Table 4, Figure 3F). A fraction enriched in this peptide was obtained for further study by C_8 RP-HPLC purification from trypsin digestion of RPTL−4VP samples. Molecular weight confirmation was obtained by MALDI, which showed the expected signal at *m*/*z* 2169.8 (internal calibration) corresponding to the singly charged molecular ion (calculated MH^+_a = 2169.5). Using the enriched fraction reconstituted in water/acetonitrile/formic acid (50/50/0.1), MS/MS on the doubly charged parent ion at *m*/*z* 1085 produced Y_3−Y_{14} and B_2−B_4 daughter ions confirming the proposed sequence of the parent peptide (Figure 3G).

Circular Dichroism of PTL. The far-UV spectrum provided information about the secondary structure of PTL. The CD spectrum demonstrated a minimum at 214 nm and crossover at about 200 nm with a positive band below 195 nm indicative of a β-sheet structure in native and reduced PTL (Figure 5). Computer-assisted analysis confirmed a predominant β-sheet structure (Table 6). Under reducing conditions ellipticity decreased in the range from 190 to 198

Table 4: Summary of the Molecular Weights of the TL Tryptic Fragments

fragment	calculated mol wt	observed molecular weights HPTL	RPTL	RPTL-4VP
19−38	2341.6_a	2341.2	2341.5	2341.7
39−44	691.3_m	691.4	NF[a]	NF
39−70	3526.0_a	3526.8	3525.5	3526.4
45−70	2852.2_a	2852.1	2852.4	2852.7
71−78	875.5_m	875.7	875.7	876.0
84−88	558.3_m	558.4	558.5	558.5
89−94	645.3_m	NF	645.4	645.7
89−101	1337.6_m	1337.7	NF	NF
95−101	710.3_m	NF	710.5	710.5
102−108	870.5_m	870.6	870.7	NF
84−108	2732.1_a	NF	2731.9	NF
102−112	1321.8_m	1320.7	1320.9	1321.3
109−112	469.3_m	NF	469.3	469.4
109−126 (Cys_{119})	2162.4_a	2162.8	NF	NF
113−129−4VP (Cys_{119})	2168.5_a	NF	NF	2168.7[c]
130−132	302.2_m	302.3	302.2	NF
133−136	443.3_m	443.2	443.3	443.3
133−155	2513.8_a	NF	2513.6[b]	NF
133−139	783.5_m	783.4	783.4	783.2
133−150	2086.1_m	NF	2087.7	2086.0
140−150	1320.6_m	1320.7	1320.9	1320.9
140−155	1746.9_m	NF	1747.8	NF
156−166	1184.7_m	1184.8	1185.4	1185.1
151−155	444.3_m	NF	444.2	NF
(79−83) + (167−176) (Cys_{79} and Cys_{171})	1612.7_m	1612.7	1613.2	1612.6

[a] NF = not found. [b] Confirmed by MS/MS (data not shown). [c] Confirmed by MS/MS, see Figure 3G.

Table 5: Summary of MS/MS Data on the DTT Released Individual Components of the Putative Disulfide Linked Fragment (C_{79}−K_{83} + Q_{167}−D_{176})[a]

obsd daughter ions	proposed assignment[b]	$calcd_m$ *m*/*z* values of the predicted daughter ions
Putative DTT Released Fragment CQEVK (C_{79}−K_{83}); Parent Ion *m*/*z* 606 (7%)		
361.4 (35%)	B_3	361.4
246.5 (20%)	Y_2	246.3
232.4 (100%)	B_2	232.3
147.5 (50%)	Y_1	147.2
Putative DTT Released Fragment QSETCSPGSD (Q_{167}−D_{176}); Parent Ion *m*/*z* 1010 (60%)		
666.2 (5%)	Y_7	666.7
635.9 (10%)	B_6	636.6
462.5 (30%)	C_4	461.4
375.5 (100%)	Y_4	375.4

[a] Both parent ions were singly charged. The (%) values refer to the relative intensity of the various ions in each mass spectrum. [b] For assignment, see Experimental Procedures. Data only list those daughter ions that could be assigned.

nm and increased from about 198 to 250 nm in the far-UV region (Figure 5). The ratio of ellipticity at 195/214 nm was 0.35 for the native form and 0.32 for the reduced form. In the presence of urea, ellipticity decreased at 209−230 nm and slightly increased at 230−242 nm. This alteration in urea was markedly enhanced by disulfide reduction (Figure 6) indicating loss of β-structure.

The near-UV CD spectra in the range from 250 to 300 nm provided information about the environment of the aromatic side chains of the protein. Comparison of the spectra of reduced PTL to native PTL demonstrated mitigation of the trough at 280 nm (Figure 7) indicating a conformational change involved aromatic residues. The

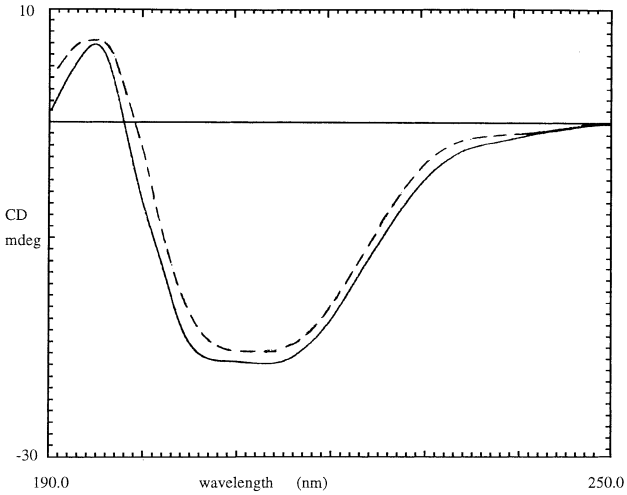

FIGURE 5: Far-UV CD spectra show the β-structure of tear lipocalin in reduced (solid line) and native (dashed line) states. The β-structure is essentially preserved. However, the generalized signal reduction of the CD spectra indicates a greater flexibility in the reduced protein.

Table 6: Estimation of α-Helix and β-Sheet Content in PTL at pH 7.3[a]

submethod	% α-helix	% β-sheet	% others
Johnson	12.8	39.9	47.3
Kabsch−Sandars	15.2	40.1	44.7
Levitt−Greer	17.2	52.5	30.3

[a] Estimation of the secondary structure was performed using protein secondary structure predictor program (Selcon) compliments of Dr. Robert W. Woody (*31*). This program predicts percent secondary structure based on iterations from analyses of X-ray crystallographic structures of other programs.

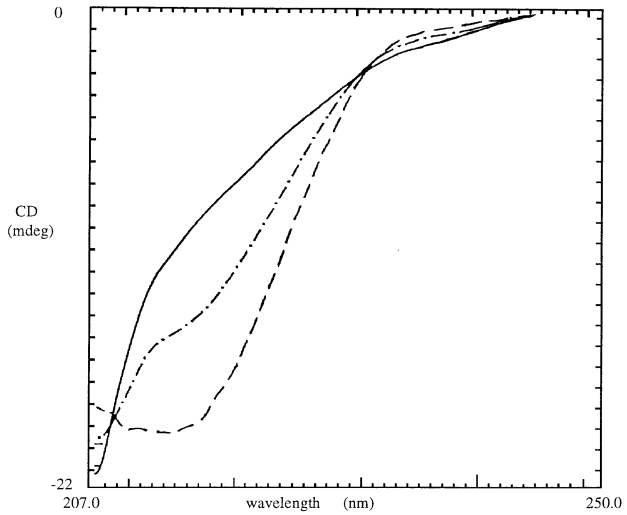

FIGURE 6: Far-UV CD spectra of PTL (dashed line), with the addition of urea (dotted and dashed line), and addition of urea + β-mercaptoethanol (solid line) demonstrate the loss of β-structure in TL with disulfide reduction in the presence of a chaotropic agent.

difference spectra (Figure 8) mimicked the spectroscopic pattern of native PTL in the near-UV region suggesting that the changes in optical activity with disulfide reduction occurred uniformly in the various aromatic side chains.

Retinol was chosen as a binding agent to study the spectra of a ligand−PTL complex because free retinol is optically inactive whereas bound retinol shows optical activity at 320−345 nm. The addition of retinol to native PTL resulted in

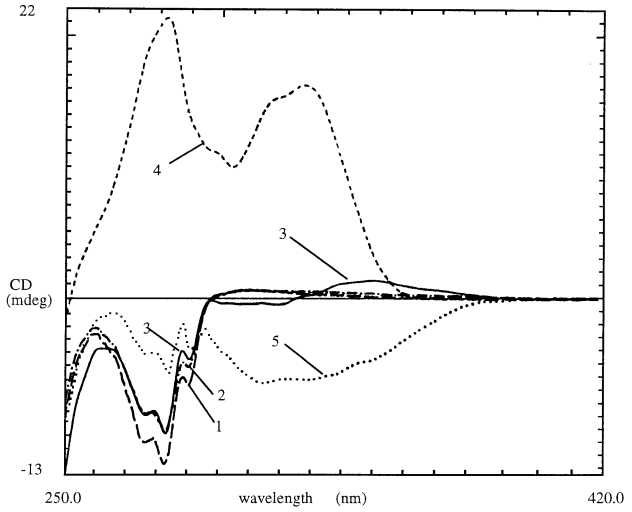

FIGURE 7: Near-UV CD spectra of PTL: native PTL (dashed line 1), reduced PTL (dotted and dashed line 2), PTL with the addition of retinol (solid line 3), reduced PTL with retinol (small dashed line 4), and delipidated PTL with retinol (dotted line 5). Reduction in the trough at 280 nm indicates that Tyr and Trp residues are involved in alteration of the TL conformation with reduction and retinol binding. Increased optical activity at 320 nm denotes greater retinol binding after disulfide reduction.

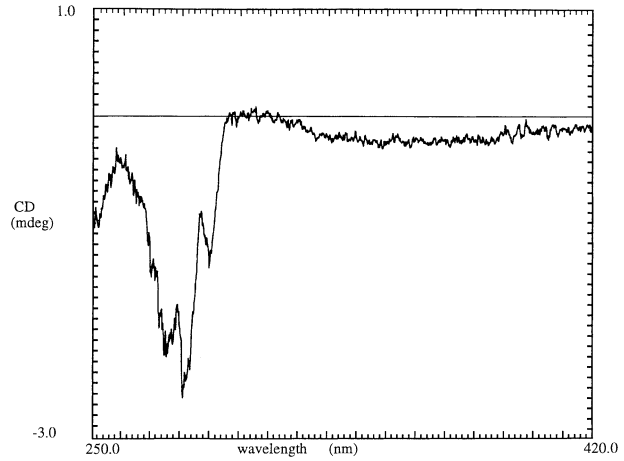

FIGURE 8: Difference CD spectra of native PTL and reduced PTL reflects the general spectra of PTL, indicating equal alteration for all aromatic residues (mainly Trp and Tyr).

the formation of a positive CD band at 345 nm (Figure 7) indicating the formation of a protein−ligand complex. The addition of retinol to delipidated PTL showed greater but negative ellipticity (Figure 7). The spectra for reduced PTL, incubated with retinol, showed an intense band with a maximum at 324 nm that was about 10 times greater than the signal observed in the native state, indicating increased binding with retinol (Figure 7). Delipidated reduced PTL and native reduced PTL featured similar spectra with retinol incubation (data not shown). Diminution of the trough at 280 nm with native PTL was observed with both reduced PTL and PTL incubated with retinol; optical activity decreased in the regions with aromatic side chains (Figure 7). The spectra for reduced PTL incubated with retinol showed that the negative aromatic signal observed with native PTL changed to a strong positive signal. The difference spectra (Figure 9) in concert with the spectra in Figure 7 demonstrated that the greatest relative alteration of optical activity with retinol added to native PTL occurred

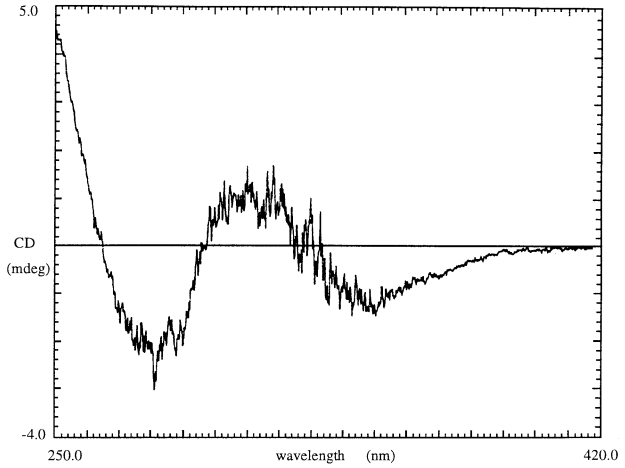

FIGURE 9: Difference CD spectra of native PTL and retinol-incubated PTL. The greatest alteration of the spectra relative to the degree of optical activity occurs in the 280−290 nm region, indicative of a conformational change involving aromatic residues.

in the region of 290 nm (indicative of the contribution of tryptophan residues, with less at 280 nm (the contribution of tyrosine and tryptophan residues) and in the region of 345 nm (the contribution of retinol). Incubation of delipidated PTL with retinol also resulted in reduction of optical activity at 290 nm when compared to native PTL (Figure 7).

DISCUSSION

We have described the precise molecular weights of the six major isoforms of TL their disulfide motif and provide direct evidence of a predominantly pleated β-sheet secondary structure for this protein. In addition, we provide evidence that structural shifts during ligand binding involve aromatic residues in TL.

Mass Measurements of the Various TL Isoforms. The agreement between measured and calculated molecular weights of the two predominant isoforms excludes the possibility of their posttranslational modification (apart from disulfide formation). These two isoforms were identified with masses that predict amino acid sequences ending with residue 176 of the putative precursor predicted from cDNA cloning. Therefore, truncation at the carboxy terminus for these isoforms is excluded. A third isoform was identified whose mass is consistent with the amino terminus of TL 18/5.2 published by Delaire et al. (*2*) with the inclusion of an additional phenylalanine residue, although we have no a priori reason for suggesting that such an inclusion occurs. ESI results revealed the presence of at least three other components in the TL preparations whose masses varied by less than or equal to 111 Da from the major isoform. In contrast to the ESI data, the various isoforms of TL were not evident during MALDI, attributable to the lower resolving power of the linear time-of-flight instrument. However, the extended mass range of this instrument allowed us to search for covalently linked TL polymers, but the amount of dimer (signal intensity about 5% of the monomer) is about the same as that for any protein run under these conditions, and the dimer signal was not diminished by prior treatment with DTT. The masses of the three less abundant TL isoforms are incongruous with mass calculations based on existing published partial sequences of TL. The unknown

species are not likely to be the result of noncovalent attachment of lipid ligands to the protein because such attachments would be destroyed by the ESI process under the conditions used, and the heterogeneity remained after protein delipidation. Because the same single cDNA precursor was independently identified by three different groups, it seems unlikely that any of the products we have identified represent translation from an undescribed cDNA precursor (*1*, *6*, *8*). Furthermore, our samples of PTL and HPTL were purified from tears collected from many subjects. Therefore, the possibility remains that these isoforms represent individual variation due to amino acid substitution and/or posttranslational modifications. Not all forms were detected in all TL preparations, supporting variance in expression of the natural isoforms of the protein.

Disulfide Reactivity. Attempts to chemically modify TL with thiol reagents to confirm the number of sulfhydryl residues and define the presence of absence of an internal disulfide were confounded somewhat by the inherent heterogeneity in the sample, the proclivity of the thiol reagents to form multiple products, and the issue of accessibility of reactive sulfhydryl groups in the native protein. Spectrophotometric determination of sulfhydryl content indicated three per molecule in the reduced/denatured protein. Molar ratios less than 1 in native protein indicate diminished accessibility of PDS and DTNB to the free sulfhydryl group. Furthermore, 4VP reacted completely with protein in tears and with highly purified protein, indicating equivalent accessibility of the one free sulfhydryl group in all preparations. DTNB is the largest of the reagents and was less reactive with native protein possibly reflecting the role of steric hindrances in these reactions. 4VP and IAA treatment of reduced denatured TL indicated three reactive sulfhydryl groups, confirming the presence of a single disulfide in the native molecule.

Trypsinization of TL. Trypsin was selected for digestion because the predicted array of fragments included several that contained a single cysteine. Other cleavage methods were excluded because of the adverse conditions for retention of the disulfide bond or because the putative fragments would not have contained single cysteines (cyanogen bromide). Computer-based molecular weight searches identified predicted trypsin fragments which accounted for 95% of the entire length of TL_{19-176}, only leaving unaccounted a tri- and a hexapeptide. Of the predicted tryptic fragments it is noteworthy that fragments encompassing Cys_{79} and Cys_{171} could not be found except in a combined form held together by a disulfide bond. The same result was obtained from minimally (one RP-HPLC step) and highly purified protein suggesting that disulfide scrambling had not taken place during the purification process. The structure of the disulfide-linked fragment was confirmed by treatment with an excess of thiol reagent, which resulted in the simultaneous generation of the two predicted fragments with the loss of the parent molecule, and by MS/MS experiments on the two fragments, which confirmed their predicted amino acid sequence. Molecular weight based computer searches found only one trypsin fragment from highly purified protein that encompassed Cys_{119} ($Ser_{109}-Lys_{126}$). However, trypsinization of protein obtained from 4VP-treated tears produced a fragment that had a measured molecular weight and MS/MS pattern of daughter ions as that predicted for the $Glu_{113}-Arg_{129}$ sequence containing pyridoethylated cysteine. This result confirms that residue 119 contains the free thiol group in the protein and confirms that protein purification did not result in any scrambling of the native disulfide linkage.

Circular Dichroism. Interpretation of far-UV experiments permit conclusions about the structure of TL. The data verify that TL have a pleated β-sheet structure as predicted from analysis of the deduced protein sequence (*1*). Estimation of secondary structure of TL demonstrates that the content of α-helix and β-structure is similar to other members of the lipocalin superfamily (*23*−*25*).

The influence of the disulfide bond on secondary structure is evident from the far-UV CD spectra (Figure 5). There is minimal alteration of the shape of the spectra under reducing conditions indicating retention of β structure.

The disulfide bond also influences urea-induced protein unfolding. Examination of the spectra (Figure 6) shows that reduction of β structure by urea alone is incomplete and markedly enhanced in the presence of both reducing and chaotropic agents. The disulfide bond prevents the complete unfolding of the protein by urea. Additional information about protein flexibility is evident from analysis of the ratio of maximum positive and negative ellipticity (195/214 nm) (*26*). It is known that the molecular asymmetry indicated by a high ratio reflects a relatively more twisted β sheet structure that is energetically more favorable and more rigid (*27*, *28*). The ratio is less for reduced TL and hence indicates that some relaxation of protein structure occurs with dissolution of the disulfide bond. Similar alterations have been observed in the CD analysis for other proteins with methods that produce a less rigid state. Bovine β-lactoglobulin, a lipocalin, shows a reduced ratio of maximum positive/negative ellipticity when the temperature is increased from 37 to 55 °C (*25*). For cardiotoxin analogue (III), an all β sheet protein, the ratio is reduced in the molten globule state induced with 3% TCA.

The influence of the disulfide bond on rigidity of the aromatic residues in TL is evident from the near-UV measurements. The general diminution in optical activity in the near-UV region indicates a more symmetric environment for aromatic side chains in the reduced than in the native state (Figure 7). In the difference CD spectra (Figure 8) fine structure is evident, reflecting the changes in conformation of aromatic residues. Previous authors have shown that if the spectroscopic changes were due solely to the reduction of the disulfide, the difference CD would show a smooth structureless line in the 250−310 nm region (*29*−*31*). Furthermore, the shapes of the spectroscopic patterns of the near-UV TL spectrum and difference spectrum after reduction are similar; hence the alteration of the original signal is proportional for all aromatic residues and indicates a general transition to a less rigid state. The aromatic amino acid residues in TL include one Trp, five Tyr, and three Phe. Because Phe has a relatively low molar extinction coefficient, the spectra disproportionately reflect Trp and Tyr.

The influence of the disulfide bond on ligand affinity for TL is evident from the analysis of optical activity generated by bound retinol (free retinol has no optical activity) in the near-UV CD spectra. The enhanced optical activity in the region of 300−340 nm indicates that retinol binds more avidly to the reduced protein than to native TL (Figure 7). Similar avid binding of retinol was observed for delipidated

reduced protein. We speculate that retinol is unable to displace the existing lipids from TL in the native state. Additional data support this conclusion. There is less retinol binding signal in CD of native TL than delipidated TL suggesting that native lipids prevent the binding of retinol. Retinol binding to delipidated TL produces a high amplitude negative CD signal, reflecting avid binding. Reduction of the disulfide bond permits a more relaxed structure that may allow displacement of native lipids by retinol. In any case, it is clear that the dissolution of the disulfide bond markedly changes the ligand binding properties of TL.

There is evidence that the conformational states of aromatic residues are influenced by the disulfide bond in ligand binding. When retinol is added to TL, there is a mitigation of the trough at 280 nm; the optical activity of the chromophore residues is altered with this ligand. The change in ellipticity is not accounted for by retinol alone since retinol has no intrinsic optical activity in this region (*20*, *32*). Disulfide reduction also produces changes in the aromatic side chains of TL. The reversal of the negative trough at 280 nm to a markedly positive CD band demonstrates retinol-induced conformational alterations of aromatic side chains in reduced TL.

It is possible to distinguish the influence of Trp from Tyr on the CD spectra. Trp has a higher molar extinction coefficient at 290 nm (4500) than Tyr (150) (*33*). Comparison of the native spectra of PTL to the difference spectra of PTL and retinol-treated PTL shows a disproportionate loss of optical activity at 290 versus 280 nm indicating that retinol binding alters the conformation of Trp more than Tyr.

The relative contribution of different ligands to asymmetry at the Trp site is discernible in Figure 7 at 290 nm. The negative CD signal of native PTL is diminished upon incubation with retinol, but the effect is greater with prior removal of native lipids. This suggests that native lipids may produce more asymmetry at the Trp site than retinol. The disulfide bond is also important. Retinol incubation of reduced TL results in marked reversal of the negative signal in the aromatic region (250−300 nm) (Figure 7) and indicates a complete change in asymmetry in the Trp site and perhaps a different mechanism of retinol binding.

Taken together, the CD data provide evidence that the disulfide bond contributes to the rigidity and asymmetry of TL and specifically involves aromatic residues but minimally alters secondary structure. The affinity of retinol for TL is markedly influenced by disulfide dissolution. An intact disulfide restricts the exposure of the hydrophobic sites in the TL cavity to retinol.

The Conserved Lipocalin Disulfide Bridge. Existing models of lipocalin structure feature a β barrel formed by eight antiparallel strands that have been labeled A−H. A unifying motif of lipocalin structure is the presence of a disulfide bond between two conserved cysteine residues. One of these occurs in a β-sheet, usually the D strand, and the other at the C terminus (*5*, *34*−*36*). Mouse urinary protein, β-lactoglobulin, retinol binding protein, insecticyanin, and bilin binding proteins have cysteine residues near the carboxy terminus, and in each case this carboxy-terminal cysteine is involved in an intramolecular disulfide bond. TL are unusual because there are only three cysteines and only one intramolecular disulfide bridge; TL are an excellent model to study the functional characteristics of this disulfide bond. One analysis of crystal structure of the lipocalin family reported that the carboxy terminus is in the cup or barrel of the molecule that binds the ligand (*5*). It is therefore plausible that the disulfide in this region influences the ligand binding site. Our data suggest that the disulfide exerts its effect through the conformational state of the aromatic site.

The disulfide bridge of TL minimally affects secondary protein structure but contributes significantly to the rigidity of aromatic sites. Because this disulfide motif is strongly conserved, the functional properties in tear lipocalins have implications for the entire lipocalin family. The disulfide bridge may play a role in the modulation of ligand-induced protein conformation changes, affect the affinity of ligands for lipocalins, and influence the release of ligand to target receptors.

ACKNOWLEDGMENT

Christopher Reyes completed the first RP-HPLC purification and ESI experiments, Richard Stevens, Ph.D., did the MALDI measurements, F. T. Ho was responsible for the CZE measurement, Farzin Feizbach helped with the trypsin purification, and Rouda Houssani and Jason Higginson helped with the 4-VP experiments.

REFERENCES

1. Redl, B., Holzfeind, P., and Lottspeich, F. (1992) *J. Biol. Chem. 267*, 20282−20287.
2. Delaire, A., Lassagne, H., and Gachon, A. M. F. (1992) *Exp. Eye Res. 55*, 645−647.
3. Fullard, R. J., Kissner, D. M. (1991) *Curr. Eye Res. 10*, 613−628.
4. Glasgow, B. J., Abduragimov, A. R., Farahbakhsh, Z., Faull, K. F., and Hubbell, W. L. (1995) *Curr. Eye Res. 14*,363−372.
5. Flower D. R. (1995) *J. Mol. Recognit. 8*, 185−195.
6. Glasgow, B. J., Heinzmann, C., Kojis, T., Sparkes, R., Mohandas, T., and Bateman, J. B. (1993) *Curr. Eye Res. 11*, 1019−1023.
7. Lassagne, H., Ressot, C., Mattei, M. G., and Gachon, A. M. F. (1993) *Genomics 18*, 160−161.
8. Bläker, M., Kock, K., Ahlers, C., Buck, F., and Schmale, H. (1993) *Biochim. Biophys. Acta 1172*, 131−137.
9. Glasgow, B. J. (1995) *Graefe's Arch. Clin. Exp. Ophthalmol. 233*, 513−522.
10. Flower, D. R. (1996) *Biochem. J. 318*, 1−14.
11. Bianco-Vaca, F., Via D. P., Yang, C.-Y., Massey, J. B., and Pownall, H. J. J. (1992) *J. Lipid Res. 33*, 1785−1795.
12. Chao, C. W., and Butala, S. M. (1986) *Curr. Eye Res. 5*, 895−900.
13. Bozimowski, D., Artiss, J. D., and Zak, B. (1985) *J. Clin. Chem. Clin. Biochem. 23*, 683−689.
14. Roepstorff, P., and Fohlman, J. (1984) *Biomed. Mass Spectrom. 11*, 601.
15. Biemann, K. (1988) *Biomed. Environ. Mass Spectrom. 16*, 99−111.
16. Lee, T. D., and Shively, J. E. (1990) *Methods Enzymol. 193*, 361−74.
17. Grassetti, D. R., and Murray, J. F., Jr. (1967) *Arch. Biochem. Biophys. 119*, 41−49.
18. Ellman, G. L. (1959) *Arch. Biochem. Biophys. 82*, 70−77.
19. Riddles, P. W., Blakeley, R. L., and Zerner, B. (1983) *Methods Enzymol. 91*, 49.
20. Heller, J., and Horwitz, J. (1973) *J. Biol. Chem. 248*, 6308−6316.
21. Hubbard, R., Brown, P. K., and Bownds, D. (1971) *Methods Enzymol.* XVIIIC, 628−629.
22. Sreerama, N., and Woody, R. W. (1993) *Anal. Biochem. 209*, 32−44.

23. Dufour, E., and Haertle, T. (1990) *Protein Eng. 4*, 185−190.
24. Muccio, D. D., Waterhouse, D. V., Fish, F., and Brouillette, C. G. (1992) *Biochemistry 31*, 5560−5567.
25. Molinari, H., Ragona, L., Varani, L., Musco, G., Consonni, R., Zetta, L., and Monaco, H. L. (1996) *FEBS Lett. 381*, 237−243.
26. Woody, R. W. (1996) In *Circular Dichroism and the Conformational Analysis of Biomolecules* (Fasman, G. D., Ed.) pp 54−55, Plenum Press, New York.
27. Chou, K.-C., Némethy, G., and Scheraga, H. A. (1983) *J. Mol. Biol. 168*, 389−407.
28. Chou, K.-C., Pottle, M., Némethy, G., Ueda, Y., and Scheraga, H. A. (1982) *J. Mol. Biol. 162*, 89−112.
29. Kosen, P. A., Creighton, T. E., and Blout, E. R. (1983) *Biochemistry 22*, 2433−2440.
30. Mayr, L. M., Willbold, D., Landt, O., and Schmid, F. X. (1994) *Protein Sci. 227*, 227−239.
31. Woody, R. W., and Dunker, A. K. (1996) In *Circular Dichroism and the Conformational Analysis of Biomolecules* (Fasman, G. D., Ed.) pp 109−157, Plenum Press, New York.
32. Adler, A. J., Evans, C. D., and Stafford, W. F., III (1985) *J. Biol. Chem. 260*, 4850−4855.
33. Demchenko, A. (**1986**) in *Ultraviolet Spectroscopy of Proteins*, pp 14−16, Springer-Verlag, New York.
34. Huber, R., Schneider, M., Mayr, I., Müller, R., Deutzmann, R., Suter, F., Zuber, H., Falk, H., and Kayser, H. (1987) *J. Mol. Biol. 198*, 499−513.
35. Cowan, S. W., Newcomer, M. E., and Jones, T. A. (1990) *Proteins: Struct. Funct. Genet. 8*, 44−61.
36. Papiz M. Z., Sawyer, L., Eliopoulos, E. E., North, A. C. T., Findlay, J. B. C., Sivaprasadarao, R., Jones, T. A., Newcomer, M. E., and Kraulis, P. J. (1986) *Nature 324*, 383−385.

BI9720888